Multi-Polarization C-Band SAR Signatures of Arctic Sea Ice

S. V. Nghiem[1] and C. Bertoia[2]

[1]Jet propulsion Laboratory, MS 300-235
California Institute of Technology
Pasadena, CA 91109
Tel: 818-354-2982, Fax: 818-393-3077
E-mail: nghiem@solar.jpl.nasa.gov

[2]U. S. National Ice Center
4251 Suitland Road, FOB 4
Washington, DC 20395
Tel: 301-457-5314, Fax: 301-457-5300
E-mail: bertoiac@natice.noaa.gov

Abstract - **The Advanced Synthetic Aperture Radar (ASAR) is scheduled to be launched on the ENVISAT satellite in summer 2001. For Arctic sea ice mapping using future ASAR data, we carry out a study of multiple polarization C-band SAR signatures of various sea ice types. We present polarimetric SAR data acquired over sea ice acquired by the Jet Propulsion Laboratory polarimetric AIRSAR system on the NASA DC-8 aircraft over sea ice regions in the Beaufort Sea and the Bering Sea. We use a physical sea ice model to study polarimetric scattering signatures of sea ice. The results also provides useful information to the future RADARSAT-2 multi-polarization SAR for sea ice mapping.**

I. INTRODUCTION

Spacebome Synthetic Aperture Radars (SAR) have been applied to operational sea ice mapping over large scales in polar oceans [1]. This paper presents results from a study of multiple-polarization C-band SAR signatures of sea ice for applications to sea ice mapping with ENVISAT ASAR data. We use actual polarimetric SAR data acquired by the JPL AIRSAR system over sea ice regions in the Beaufort Sea and the Bering Sea. We use a physical sea ice model to obtain polarimetric scattering signatures of several sea ice types. The model results are verified by comparisons with AIRSAR data for the different ice types. Based on geophysical parameters characterizing sea ice, the sea ice model is then used to obtain multiple polarization signatures of sea ice under various conditions. Sea ice backscatter values are calculated at the multiple polarizations over the incidence angle range of ENVISAT ASAR to determine how to exploit the new features of ENVISAT data. The results are also useful to investigate sea ice mapping with the future RADARSAT-2 SAR, which is designed for multi-polarization SAR [2].

II. JPL AIRSAR DATA OVER SEA ICE

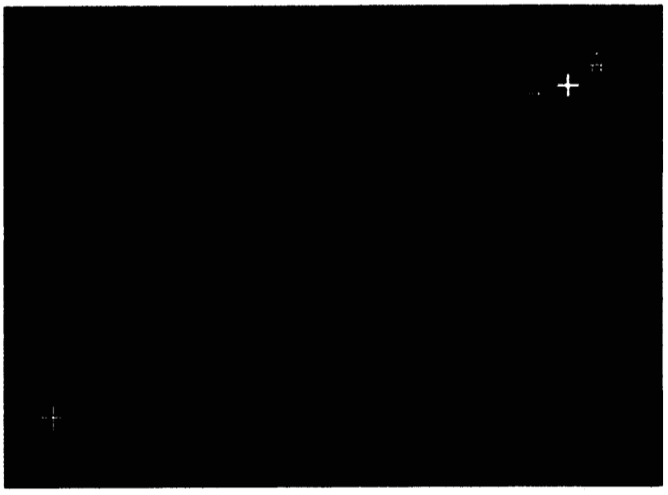

Fig. 1. Location of seven JPL AIRSAR sea ice scenes.

The research performed at the Jet Propulsion Laboratory, California Institute of Technology (S.V.N.) was sponsored ny the National/Naval Ice Center through an agreement with the National Aeronautics and Space Administration.

The NASA DC-8 aircraft carrying the JPL polarimetric *AIRSAR* system were deployed to collect data over sea ice in March 1988. Numerous sea-ice *SAR* scenes were acquired in the Beaufort and in the Bering Sea. The *SAR* scene locations are plotted in Figure 1 over the region bounded by latitudes 54% and 77% and longitudes 173°W to 137°W. An example of sea ice image for *AIRSAR* Scene 0125 is shown in the right panel of Figure 2. The color in Scene 0125 is the red-green-blue composite representing the backscatter intensity at P (red), L (green), and C (blue) bands. We use data from seven different scenes taken by the JPL polarimetric *AIRSAR* system over sea ice.

Fig. 2. Example of sea ice image by JPL *AIRSAR*.

III. SEA ICE CHARACTERISTICS

At the time of the JPL *AIRSAR* deployment corresponding to the transition from winter to spring in March 1988, the sea ice cover was extensive and covered much of the Beaufort Sea. The ice edge was extended down in the Bering Sea to the vicinity of 57°N latitude in the south of Nunivak Island, Alaska. This sea ice cover condition is observed in the ice chart [3] in Figure 3 presenting the synoptic view of Arctic sea ice. The ice charts are derived by the National Ice Center primarily from the Advanced Very High Resolution Radiometer (AVHRR) sensor aboard NOAA satellites and the Operational Line Scan (OLS) sensor carried by the Defense Meteorological Satellite Program satellites (Benner, 2000). In Figure 2, the ice charts are for week 12 of 1988 about the time period of the *AIRSAR* data acquisitions.

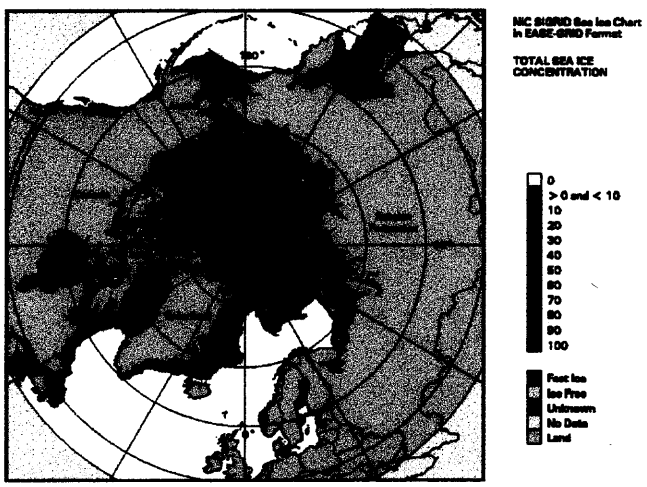

Fig. 3. National Ice Center 7-day ice charts showing Arctic sea ice cover in terms of total sea ice concentration.

These scenes contain various ice types including multi-year ice, first-year ice with different thickness and age, and newly formed lead ice. An ice camp was located at the edge of a multi-year ice floe, adjacent to a frozen lead containing thick first-year sea ice. Sea ice characterization data and environmental conditions were recorded at the ice camp and used in the analysis of *AIRSAR* data.

IV. SEA ICE AND OCEAN MODELS

Polarimetric backscatter model have been developed for sea ice over the past decade and model results have been compared and verified with measurements in laboratory conditions and Arctic field environments [4]. The model is derived from the first principle from Maxwell's equations under the framework of the analytic wave theory. The theory preserves phase information which is necessary to calculate polarimetric backscatter signatures of sea ice. Snow-covered sea ice is modeled with a multi-layer configuration with composite rough interfaces.

For ice-free ocean, empirical geophysical model function CMOD3-H1 relates co-polarized backscatter at the vertical polarization (σ_{VV}) with neutral wind speed and direction at 10-m height [5]. The model results compared well with airborne C-band radar measurements obtained during the Surface Wave Dynamics Experiment in the moderate wind speed range [6]. Co-polarized backscatter ratio $\gamma=\sigma_{VV}/\sigma_{HH}$ can be

calculated from a two-scale [7], which is larger than measured data. To match with ocean backscatter ratio measured by AIRSAR, we apply a modification factor as a function of incidence angle, to the model calculated value of γ.

V. RESULTS

Results show that co-polarized backscatter can be used to distinguish different ice types; however, the single polarization backscatter cannot be used to classify ice cover and ice-free ocean consistently over different wind speeds. An exception is the image swath 1 (IS1) where σ_{VV} can be used to map various sea ice types and ice-free ocean at different wind speeds. Various polarization combinations in all Alternating Polarization (AP) modes on ENVISAT ASAR are investigated for the sea ice mapping with different swaths. The AP W-VH mode with both σ_{VV} and σ_{VH} measurements is suggested for IS1-IS3 swaths subject to future field validation experiments. The AP HH-W mode can be used over IS5-IS7 swath for a more robust results of sea ice and ocean identification and classification. The IS4 swath may be used for the mapping with some limitations due to the confusion between first-year ice and Ocean at low winds.

ERS-1 SAR data together filed data and model results show that temperature changes such as the diurnal effects in late winter or spring in the Arctic can have significant effects on backscatter even before any melting occurs. Thus, ENVISAT ASAR data acquired in ascending and descending orbits at different times of the day need to be analyzed separately to obtain consistent results for sea ice mapping. Note that this paper considers sea ice conditions without melting. During the transition periods, sea ice backscatter signatures become complicated due to the phase changes in the melting processes. These variations requires temporal data to analyze sea ice backscatter signatures. In summer, sea ice surface is wet and multi-polarization backscatter signatures for sea ice and ocean are overlapping. In this case, statistical analyses are necessary for the sea ice mapping.

Covering a wider strip of 405 km, the ENVISAT ASAR Wide Swath (WS) mode is more appropriate to the global monitoring mission of the National Ice Center. The total swath in this mode is a combination of five subswaths using the ScanSAR technique. However, the WS mode forces a choice of backscatter data acquisition at a single polarization, either σ_{HH} or σ_{VV}. With the analysis described in this paper for different modes at different IS swaths, we can determine the ice mapping capability and limitations at different incidence angles and polarizations throughout the entire ScanSAR swath. Further research needs to be conducted using seasonal wind field distributions, either modeled or from satellite scatterometer observations, in conjunction with ice type distribution from the National Ice Center's climatological database of sea ice charts. Such work will help select the appropriate polarization to optimize the performance for ice mapping with single-polarization ScanSAR data at different seasonal times and over different regions of the Arctic.

REFERENCES

[1] C. Bertoia, J. Falkingham, and F. Fetterer, "Polar SAR data for operational sea ice mapping," in *Analysis of SAR Data of the Polar Oceans*, pp. 201-234, Berlin, Germany: Springer-Verlag, 1998.

[2] P. Meisl, A. Thompson, and A. Luscombe, "RADARSAT-2 Mission: Overview and development status," *Proc. EUSAR*, Munich, Germany, 2000.

[3] Environmental Working Group, *Joint U.S. Russian Sea Ice Atlas* [CD Vers. 1.01, Boulder, Colorado: NSIDC/CIRES, University of Colorado, 2000.

[4] S.V. Nghiem, R. Kwok, S.H. Yueh, and M.R. Drinkwater, "Polarimetric signatures of sea ice, 1, Theoretical model," *Joumal of Geophysical Research*, vol. 100, no. C7, 13665-13679, 1995.

[5] A.E. Long, "C-band V-polarized radar sea echo model from ERS-1 Haltenbalken Campaign," in *Proc. URSZ Microwave Signature Conference*, IGLS-Innsbruck, Austria, 1992.

[6] S.V. Nghiem, F.K. Li, S.H. Lou, G. Neumann, R.E. McIntosh, S.C. Carson, J.R. Carswell, E.J. Walsh, M.A. Donelan, and W.M. Drennan, "Observations of ocean radar backscatter at Ku and C bands in the presence of large waves during the Surface Wave Dynamics Experiment," *ZEEE Transactions on Geoscience and Remote Sensing*, vol. 33, no. 3, pp. 708-721, 1995.

[7] W.J. Plant, "A two-scale model of short wind-generated waves and scatterometry, *Joumal of Geophysical Research*, vol. 91, no. C9, pp. 10735-10749, 1986 (corrected 1988).